Effects of Self Stress on the Transport of Guest Species in Solids: Transport of Hydrogen in Metals

ARTICLE *in* THE JOURNAL OF PHYSICAL CHEMISTRY B · APRIL 2002

Impact Factor: 3.3 · DOI: 10.1021/jp013946j

Effects of Self Stress on the Transport of Guest Species in Solids: Transport of Hydrogen in Metals

Bartlomiej Legawiec and Piotr Zoltowski*

Institute of Physical Chemistry of Polish Academy of Sciences, Kasprzaka 44/52, 01-224 Warsaw, Poland

Received: October 25, 2001; In Final Form: February 28, 2002

Influence of self stress on the transport of a guest in a host matrix is studied within the process of hydrogen permeation through a large thin membrane having properties similar to those of palladium or $Pd_{81}Pt_{19}$ alloy. The equilibrium in the system is perturbed at one side of the membrane by a sinusoidal signal of hydrogen concentration. At the opposite side, the hydrogen concentration is maintained at its initial value, and the flux of hydrogen is the response. The transport equations are solved numerically for a wide range of frequencies and amplitudes of the perturbing signal. At the periodic steady state, the larger the signal amplitude, the more important become the zero and higher harmonics of the flux, accompanying the fundamental harmonics. The presence of the zero harmonics causes a permanent pumping of hydrogen throughout the membrane. The fundamental harmonics closely reproduces the results obtained by solving the linearized transport equations. This means that, up to the largest amplitudes, the frequency spectrum of the fundamental harmonics allows for obtaining reliable values of the diffusion coefficient of hydrogen and the bulk elastic modulus of the metal matrix.

1. Introduction

Elastic host matrixes expand when accepting a guest. Thus, the nonuniform distribution of a guest induces mechanical self stress in the system. On the other hand, the stress is one of the factors determining the chemical potential of components of a solid system.[1] So, the stress resulting from a gradient of a guest concentration affects the guest transport within the host. This is an important feedback in phenomena involving the transport of any guest in a solid host matrix, for example, intercalation processes and transport of ions in polymers.[2,3]

Metal−hydrogen (M−H) systems are the best known host−guest systems.[4,5] The influence of stress on transport of hydrogen in metals was studied most extensively.[1,6−16] The M−H systems offer the opportunity to study this phenomenon in a coherent host matrix of simple geometry. In particular, the system can be free of phase transitions, foreign-phase inclusions, grain boundaries, and other complications, which usually occur in other host−guest systems. Hence, a M−H system may be considered as a convenient model for an analysis of transport in host−guest systems.

The chemical potential of the interstitial hydrogen in a solid metal matrix, μ, depends on the hydrogen concentration, c, and the stress, σ:[1,10,11,13]

$$\mu = \mu(0,c) - V\sigma \tag{1}$$

where $\mu(0,c)$ denotes chemical potential of hydrogen in the stress-free state ($\sigma = 0$), V is the partial molar volume of hydrogen in the matrix, and σ (below referred to as "stress") is the trace of the stress tensor induced by the presence of hydrogen in the matrix ($\sigma = \sigma_{xx} + \sigma_{yy} + \sigma_{zz}$). So, σ is the hydrostatic part of this tensor, and an analogue of hydrostatic pressure. In accordance with experimental data,[17] V is assumed to be independent of hydrogen concentration.

In comparison with the rate of the Fickian transport, the stress induced by a local gradient of hydrogen concentration is transmitted within the whole volume of elastic solid with the velocity of sound, that is, immediately. Therefore, local and nonlocal effects are observed, the former enhancing typical diffusion and the latter responsible for the so-called "uphill diffusion".[6−9]

For simplicity, we assume that the activity of hydrogen in a metal matrix equals its concentration (c) and the diffusion coefficient of hydrogen, D, is independent of c. We consider transport of hydrogen through a continuous large thin flat membrane specimen. Consequently, the transport becomes one-dimensional.

From eq 1, it follows that the flux of hydrogen, J, diffusing in the bulk of metal in response to a gradient of the chemical potential of hydrogen along the z coordinate is[1,10,11,13]

$$J = -D\left(\frac{\partial c}{\partial z} - \frac{Vc}{RT}\frac{\partial \sigma}{\partial z}\right) \tag{2}$$

where R and T denote gas constant and temperature, respectively.

To solve eq 2, the relationship between the gradients of c and σ has to be defined. A common method is to use the analogy to the effect of thermostress on conduction of heat resulting from thermal expansion of the elastic matrix. A feedback relation between the two gradients in the matrix is obtained:[1,10,11,13]

$$\frac{\partial \sigma}{\partial z} = -\frac{2}{3}\bar{V}\bar{Y}\left[\frac{\partial c}{\partial z} - \frac{12}{L^3}\int_0^L \overline{\Delta c}\left(z - \frac{L}{2}\right) dz\right] \tag{3}$$

where $\bar{Y} = \bar{E}/(1 - \nu)$ ($\bar{E}$ is the Young modulus, and ν is the Poisson ratio) denotes the bulk elastic modulus of the solid and $\overline{\Delta c} = c - c_{eq}$ is the difference between the hydrogen concen-

* To whom correspondence should be addressed. Tel: +48 (22) 632 3221 ext. 3282. Fax: +48 (22) 632 5276. E-mail: pizolt@ichf.edu.pl.

10.1021/jp013946j CCC: $22.00
Published on Web 04/24/2002

tration (c) and the initial equilibrium concentration of hydrogen in the system, c_{eq}. Obviously, c_{eq} is the reference stress-free concentration.

From eqs 2 and 3, the following flux equation results:[1,10,11,13]

$$J = J_{loc} + J_{nloc} = -D(1 + Ac)\frac{\partial c}{\partial z} + cD\frac{12A}{L^3}\int_0^L \overline{\Delta c}\left(z - \frac{L}{2}\right) dz \quad (4)$$

where

$$A = \frac{2V^2\bar{Y}}{3RT} \quad (5)$$

$$J_{loc} = -D(1 + Ac)\frac{\partial c}{\partial z} \quad (6)$$

$$J_{nloc} = -cD\frac{12A}{L^3}\int_0^L \overline{\Delta c}\left(z - \frac{L}{2}\right) dz \quad (7)$$

The flux component J_{loc} (eqs 4 and 6) is Fickian in character; the diffusion is enhanced only by local effect of stress, this being proportional to the local concentration of hydrogen. In contrast, the J_{nloc} component (eqs 4 and 7) has formally the character of a convectional flux. The integral depends on the asymmetry of hydrogen distribution in the whole membrane specimen with respect to the symmetry plane ($L/2$). The term proportional to the local concentration of hydrogen (c) may be considered the mobility of hydrogen.[11]

The calculation of J and its components (eqs 4−7) needs the knowledge of the concentration of hydrogen within the specimen. This results from the balance equation:[1,10,11,13]

$$\frac{\partial c}{\partial t} = D\left\{\frac{\partial}{\partial z}\left[(1 + Ac)\frac{\partial c}{\partial z}\right] - \left[\frac{12A}{L^3}\int_0^L \overline{\Delta c}\left(z - \frac{L}{2}\right) dz\right]\frac{\partial c}{\partial z}\right\} \quad (8)$$

The first term within the braces is a Fickian one for the effective diffusion coefficient dependent on local concentration, and the second corresponds to the convectional flux. Equation 8 is quite complex itself. Moreover, in the classical transient break-through experiment (TBT) on the effects of stress on hydrogen transport,[6−16] at both sides of the specimen the boundary conditions change in time. Nevertheless, eq 7 describes correctly the results of TBT experiments with the $Pd_{81}Pt_{19}$ specimen in the first period (up to more than 10 min in the applied experimental conditions), when the magnitude of output signal, opposite to input one, increases monotonically.[10,11]

The electrochemical impedance spectroscopy (EIS) was also proposed for the purpose of studying the effect of stress on the sorption of hydrogen into the metal electrode[18,19] and its diffusion in the bulk metal.[19] Unfortunately, within this technique, the input and output signals are measured at the same electrode surface. Thus, the nonlocal effect of stress on hydrogen diffusion cannot be observed.[19,20]

Recently, the transfer function (TF) spectroscopy has been applied for studying the diffusion of hydrogen in metals.[21−27] In contrast to EIS, TF may allow for taking into account the stress, and the dependence of the diffusion coefficient of hydrogen on hydrogen concentration in stressed M−H systems and similar dependence of the bulk elastic modulus can be measured.[25,26] As in TBT, the TF system consists of a membrane specimen separating two chambers, and similarly as in TBT before applying the step signal, it is close to equilibrium at a nonzero concentration of hydrogen (c_{eq}). At one surface ($z = 0$), the equilibrium is perturbed by a sinusoidal input signal of hydrogen concentration, $\delta c_{(0)}$, small in magnitude:[25,26]

$$\delta c_{(0)} = \Delta c_{(0)} \exp(st) \quad (9)$$

where $\Delta c_{(0)}$ denotes amplitude, t is time, and $s = i\omega$; i is the imaginary unit ($i = \sqrt{-1}$) and ω is angular frequency ($\omega = 2\pi f$, f being frequency). In the successive measurements, f is changed gradually within a range several orders of magnitude wide.

The small value of $\Delta c_{(0)}$ allows for applying the following relation:[25,26]

$$c_{eq} + |\delta c_{(0)}| \approx c_{eq} \quad (10)$$

Because of eq 10 and taking eq 9 into account, eqs 4 and 8 can be linearized:[25,26]

$$\delta J = \delta J_{loc} + \delta J_{nloc} = -D(1 + Ac_{eq})\frac{d\delta c}{dz} + c_{eq}D\frac{12A}{L^3}\int_0^L \delta c\left(z - \frac{L}{2}\right) dz \quad (11)$$

$$D(1 + Ac_{eq})\frac{d^2\delta c}{dz^2} - s\delta c = 0 \quad (12)$$

Equations 11 and 12 were solved analytically for periodic steady state at the appropriate boundary conditions for the flux (TF_f) or concentration (TF_c) TF experiments.[25,26] In case of TF_f, these were[25]

$$\delta c_{(z=0)} = \Delta c_{(0)} \exp(st) \quad \text{and} \quad \delta c_{(z=L)} = 0 \quad (13)$$

It should be emphasized that for a reliable investigation of the influence of stress on transport of hydrogen it is crucial to maintain $c_{(L)} = c_{eq}$.[25,26]

The (linear) TF_f H_l, that is, the ratio of the linear response flux signal (at $z = L$) to the concentration input signal (at $z = 0$), is as follows:[25]

$$H_l = \frac{\Delta J_{(L)}}{\Delta c_{(0)}} = D\left\{q\frac{(1 + Ac_{eq})}{\sinh(qL)} - c_{eq}\frac{12A}{q^2L^3}\left[\left(\frac{qL}{2}\right)\coth\left(\frac{qL}{2}\right) - 1\right]\right\} \quad (14)$$

where

$$q = \sqrt{\frac{s}{D(1 + Ac_{eq})}} \quad (15)$$

The first and second terms in the curly braces at the right-hand side of eq 14 correspond to local and nonlocal components of the response flux (eqs 4 and 11), respectively. Hence, similar to the flux, H_l is the sum of two coupled terms, the local one ($H_{l(loc)}$) and the nonlocal one ($H_{l(nloc)}$).[25]

In the process of penetration of the specimen, the periodic signal of hydrogen concentration is strongly attenuated. To obtain at $z = L$ a high signal-to-noise ratio, the amplitude of initial signal should be relatively large. On the other hand, the small amplitude is required (eq 10) for linearization of the transport equations (eqs 11 and 12).[25,26] If it is too large, H_l (eq 14) will depend on it, that is, the measured quantity will not exactly equal the (linear) TF_f.[25] Hence, the magnitude of the initial signal is crucial for the reliability of results of an experiment. This is a general issue in the application of small-signal techniques to nonlinear systems.

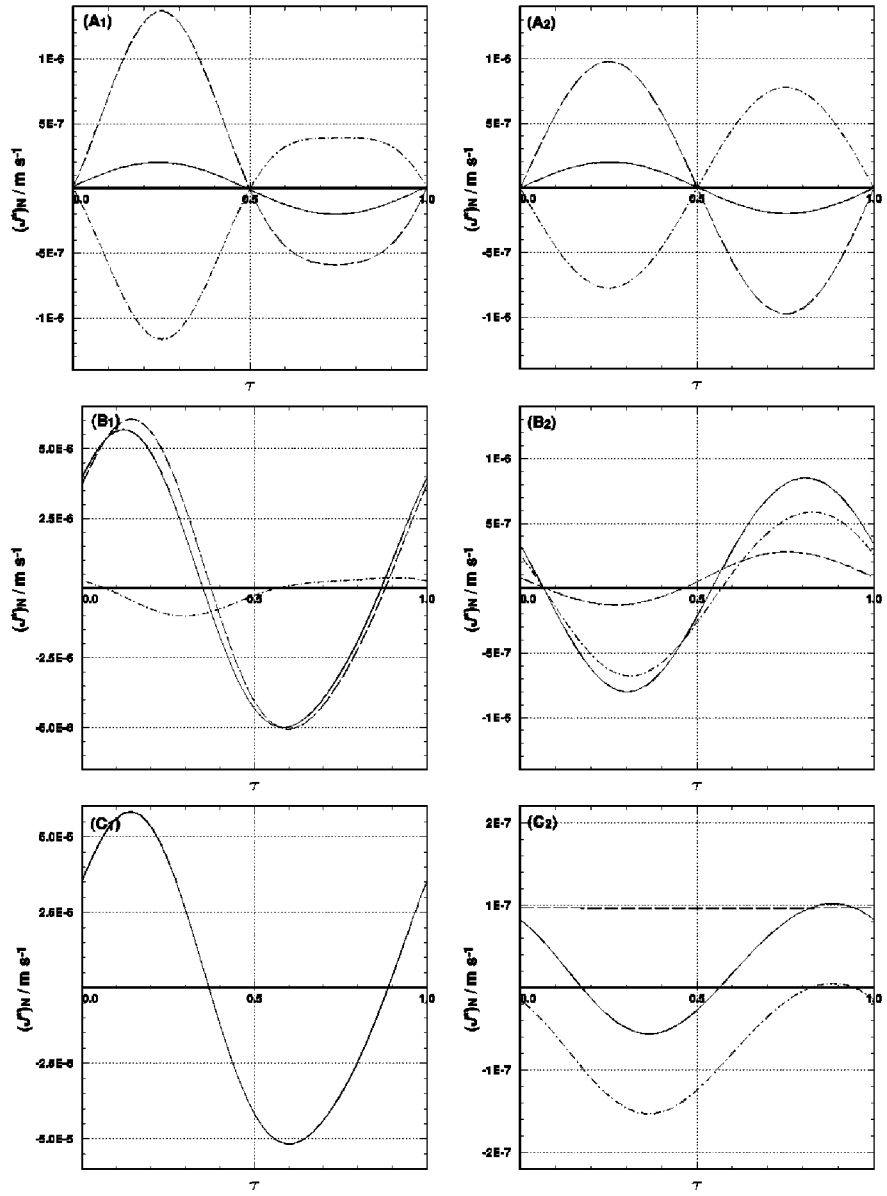

Figure 1. Plots of the periodically steady-state flux (J (—)) and its local (J_{loc} (− − −)) and nonlocal (J_{nloc} (− · −)) components (denoted jointly as J^*), calculated from eqs 4−8 at the boundary conditions defined by eq 16, vs the reduced time (τ). J^*'s are normalized with respect to $\Delta c_{(0)}$ ($(J^*)_N = J^*/\Delta c_{(0)}$). Common parameters of the system are as follows: $V = 1.77 \times 10^{-6}$ m^3 mole^{-1}; $Y = 1.844 \times 10^{11}$ Pa; $D = 1 \times 10^{-11}$ m^2 s^{-1}; $L = 5 \times 10^{-5}$ m; $T = 298.2$ K. Other parameters include the following: $c_{\mathrm{eq}} = 2.5 \times 10^4$ mole m^{-3} and $\Delta c_{(0)} = 0.5 c_{\mathrm{eq}}$. Plots A_1 to C_1 and A_2 to C_2 represent data at the input and output sides of the specimen, respectively. Plots A_1 and A_2, B_1 and B_2, and C_1 and C_2 are for f equal to 1×10^{-4}, 1×10^{-1}, and 1×10^{1} Hz, respectively.

The aim of this paper is to analyze the influence of self stress on transport of hydrogen in a solid metal matrix as described by eq 8, which is definitively nonlinear, in contrast to the Fickian transport. The analysis is performed under the same conditions that have been described recently for the (linear) TF_f[25] with the exception of the amplitude of perturbing signal. This is gradually changed in wide limits. The results are compared with those of the (linear) TF_f analysis.[25]

Similarly as it has recently been made in TF analysis,[25,26] our analysis is performed for an α-phase M−H system of properties similar to those of Pd−H and $Pd_{81}Pt_{19}$−H. As in TBT,[1,10,11] EIS,[18,19] and (linear) TF,[25,26] the membrane specimen is a large thin plate of a continuous solid.

2. Methodology

Equation 8 was solved numerically in the time domain, under the initial and boundary conditions equivalent to those applied in TF_f analysis (eq 13):[25]

$$\text{at} \quad t = 0 \qquad c_{(0 \le z \le L)} = c_{\mathrm{eq}} > 0$$

$$\text{at} \quad t > 0 \qquad c_{(0)} = c_{\mathrm{eq}} + \Delta c_{(0)} \sin(\omega t) = c_{\mathrm{eq}} + \Delta c_{(0)} \sin(2\pi\tau) \quad \text{and} \quad c_{(L)} = c_{\mathrm{eq}} \tag{16}$$

where τ denotes the reduced time defined as a fraction of 2π ($0 \le \tau \le 1$).

The following parameters were commonly assumed for the M−H system (the same as for TFs):[25,26] $V = 1.77 \times 10^{-6}$ m^3 mole^{-1},[17,28,29] $Y = 1.844 \times 10^{11}$ Pa,[30] $D = 1 \times 10^{-11}$ m^2 s^{-1} (close to this value for $Pd_{81}Pt_{19}H_n$, and three times smaller than for α-PdH_n),[9,10,12,14,20,31−36] $L = 5 \times 10^{-5}$ m (as for Pd and $Pd_{81}Pt_{19}$ specimens in EIS),[19,20] and $T = 298.2$ K. As in the (linear) TF_f analysis,[25] the explored spectrum of frequencies was $1 \times 10^{-4} \le f \le 1 \times 10^{1}$ Hz.

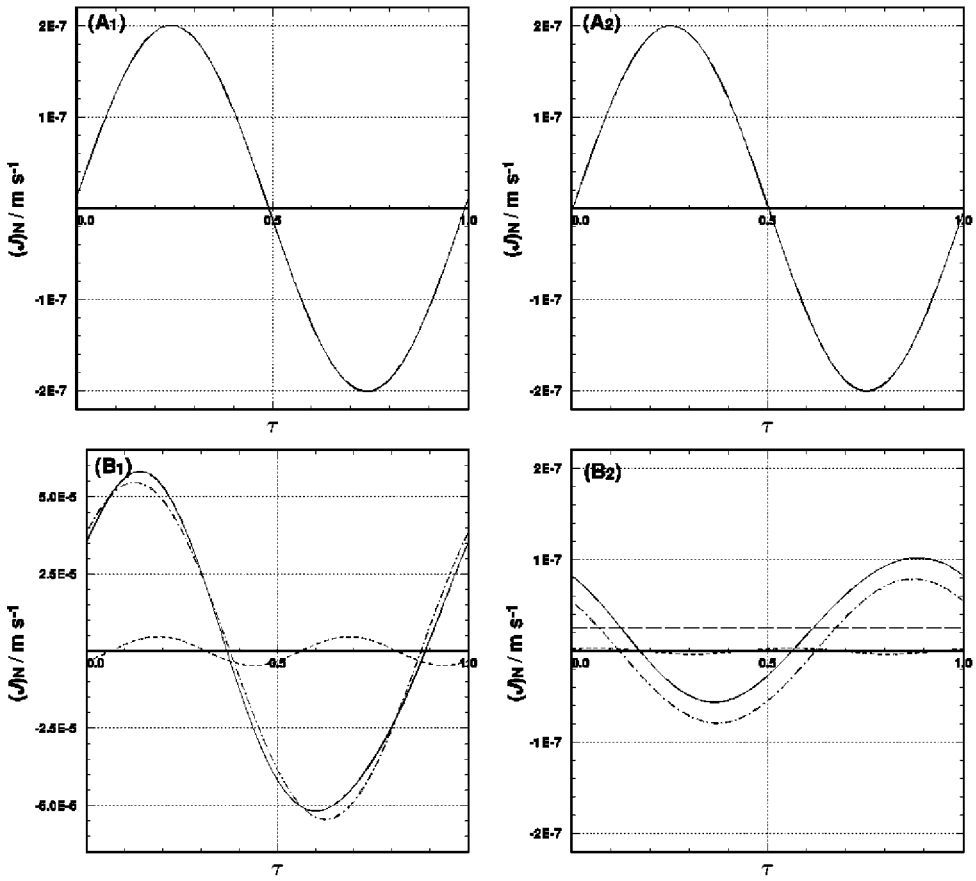

Figure 2. Plots of the results of expansion of the $(J)_N$ (see Figure 1) in the Fourier series (eq 17) vs the reduced time (τ): (—) original curves; (— — —) zero harmonics; (-·-·-·) first harmonics; (- - -) second harmonics. Plots A_1 and B_1 and plots A_2 and B_2 are at the input and output sides of the specimen, respectively. Plots A_1 and A_2 and plots B_1 and B_2 are for f equal to 1×10^{-4} and 1×10^{1} Hz, respectively (see plots A_1 and A_2 and C_1 and C_2 in Figure 1).

Two values of c_{eq} were used: 2.5×10^4 and 2.5×10^2 mole m^{-3}. The first value is close to the largest concentration of hydrogen observed in $Pd_{81}Pt_{19}$—H at room temperature (n in MH_n equal to ca. 0.2),[9,20,37,38] and the other is about 1 order of magnitude smaller than the maximal concentration in the α-PdH_n under the same conditions.[20,32,39,40] The following values of $\Delta c_{(0)}$ were applied: 0.1%, 1%, 10%, and 50% of c_{eq}.

In solving eq 8, the Crank—Nicolson method was used.[41] The integral was evaluated by the Simpson method. In the numerical scheme, the mesh sizes for length and time were 1/1000 of L, and 1/2000 of τ, respectively (the same results were obtained with twice larger mesh sizes). The computations were carried out over several hundreds of periods, until a periodic steady state was attained. Namely, they were terminated when at τ equal to 0, 0.25, 0.5, and 0.75 the relative maximal magnitude of the change of hydrogen concentration in the successive iterations, ϵ, was equal to or smaller than 1×10^{-10}.

J, J_{loc}, and J_{nloc}, each denoted below as J^*, were calculated only for $z = 0$ and $z = L$, using eqs 4—7. Then, they were subjected to the harmonic analysis. For this purpose, the Fourier series was used:

$$J^* = J^*_{0har} + \sum_{m=1}^{k} [\Delta J^*_m \sin (m2\pi\tau + \varphi^*_m)] \qquad (17)$$

where J^*_{0har}, ΔJ^*_m and φ^*_m denote the zero harmonics, the amplitude, and the phase angle of the mth term of the Fourier series, respectively.

Irrespective of its analysis, J_{0har} was used for the validation of the particular solutions of eq 8 for given sets of c_{eq}, $\Delta c_{(0)}$, and f values, against the mass balance in the system. Namely, if $|(J_{0har})_{(0)} - (J_{0har})_{(L)}|/(c_{(0)}c_{eq})$ was larger than 1×10^{-14} m^4 $mole^{-1}$ s^{-1}, the given solution of eq 8 was not accepted. To fulfill the above requirement, some calculations had to be repeated under the terminative condition $\epsilon \leq 1 \times 10^{-12}$.

Two parameters were used as a measure of relative magnitudes of individual harmonics of J at the input and output sides:

$$P_{0har} = \frac{J_{0har}}{(\sum_{i=1}^{n} |J_i - J_{0har}|)/n} \qquad (18)$$

$$P_{mhar} = \frac{\sum_{i=1}^{n} |J_i - J_{0har} - \sum_{k=0}^{m-1} J_{i,k}| - \sum_{i=1}^{n} |J_i - J_{0har} - \sum_{k=1}^{m} J_{i,k}|}{\sum_{i=1}^{n} |J_i - J_{0har}|} \qquad (19)$$

where n denotes the number of τ meshes and $J_{i,k} = 0$ for $k = 0$; $0 \leq P_{0har} \leq \infty$; $0 \leq P_{mhar} \leq 1$. The denominator in eq 18 is equivalent to the root-mean-square (rms) of the oscillating component of the flux. Hence, P_{0har} is the ratio of magnitudes of the constant and the oscillating component of the flux, and P_{mhar} is the share of particular harmonics in the oscillating component.

3. Results and Discussion

In this section, the fluxes (J^*) were normalized with respect to $\Delta c_{(0)}$ ($(J^*)_N = J^*/\Delta c_{(0)}$). In Figure 1, the fluxes $(J^*)_N$ at both

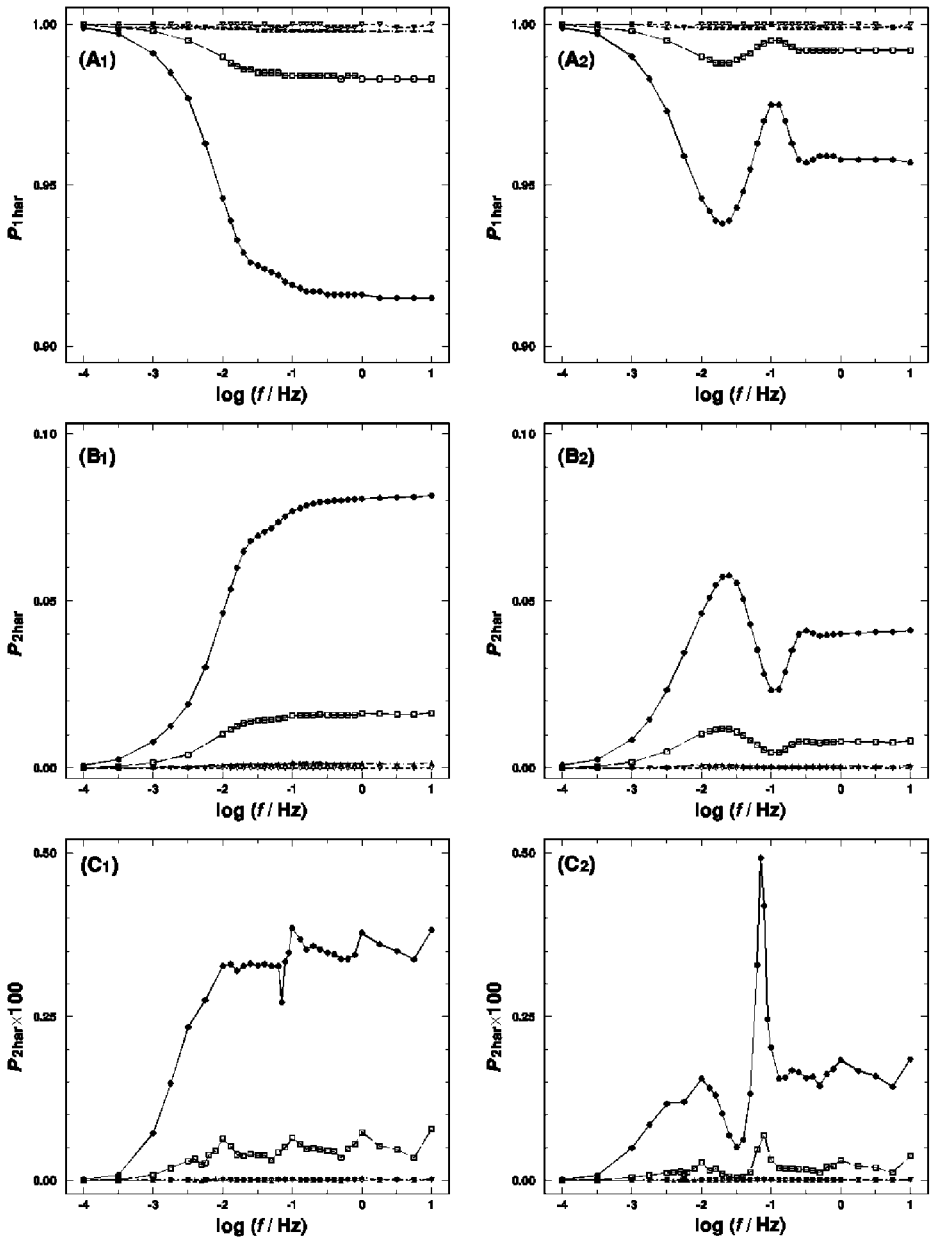

Figure 3. Plots of the share of particular (m) harmonics of the flux (J) in its oscillating part ($P_{m\text{har}}$, eq 19) vs log f: (●) $\Delta c_{(0)} = 0.5c_{\text{eq}}$; (□) $\Delta c_{(0)} = 0.1c_{\text{eq}}$; (▲) $\Delta c_{(0)} = 0.01c_{\text{eq}}$; (▽) $\Delta c_{(0)} = 0.001c_{\text{eq}}$. Plots A_1 to C_1 and plots A_2 to C_2 are at the input and output sides of the specimen, respectively. The common parameters of the system are the same as those in Figure 1. Plots A_1 and A_2 represent the first harmonics, and plots B_1 and B_2 represent the second harmonics at $c_{\text{eq}} = 2.5 \times 10^4$ mole m^{-3}; plots C_1 and C_2 represent the second harmonics at $c_{\text{eq}} = 2.5 \times 10^2$ mole m^{-3}.

sides of the specimen are plotted vs the reduced time (τ) for the larger c_{eq} and the largest $\Delta c_{(0)}$ for three different frequencies. For $f = 0.1$ mHz, at both specimen sides $(J)_N$ is the same, and its shape is close to that of a simple sinusoid (plots A_1 and A_2), as it should be if the transport will be linear. At the low frequency, the system is close to the thermodynamic steady state, in which stress is absent.[10,11,25,42−44] Both components of $(J)_N$ at $z = 0$ and $z = L$ are not sinusoidal, and $(J_{\text{loc}})_N$ is in phase and $(J_{\text{nloc}})_N$ is opposite in phase with respect to $(J)_N$ (see eqs 6 and 7). However, the specific features of $(J_{\text{loc}})_N$ and $(J_{\text{nloc}})_N$ compensate each other.

At $f = 10$ Hz, the situation is different (plots C_1 and C_2). At both specimen sides, $(J)_N$ is sinusoidal, as at $f = 0.1$ mHz, but it has a positive constant component. At $z = 0$, the amplitude of $(J)_N$ is larger by more than 2 orders of magnitude than at 0.1 mHz (plot A_1) and there is a distinct phase shift. As the initial signal penetrates the specimen, it is damped. Consequently, at $z = L$, $(J)_N$ is attenuated by more than 1 order of magnitude and shifted by ca. $\pi/2$, as compared with $z = 0$. Apparently, at $z = 0$, $(J_{\text{loc}})_N \approx (J)_N$, and at $z = L$, it oscillates around a negative constant value, while $(J_{\text{nloc}})_N$ is zero and a positive constant, respectively. At intermediate frequencies (for $f = 0.1$ Hz, see plots B_1 and B_2), the characteristic of $(J^*)_N$ falls between the two limits. Both, at $z = 0$ and $z = L$, the smaller $\Delta c_{(0)}$, the smaller are the deviations of $(J^*)_N$ from the shape of a sinusoid. The influence of c_{eq} is similar.

In Figure 2, the flux $(J)_N$ at the larger c_{eq} and $\Delta c_{(0)} = 0.5c_{\text{eq}}$ is presented as expanded into the Fourier series. For $f = 0.1$ mHz, $(J)_N$ is apparently described only by the first (fundamental) harmonics at both values of z (plots A_1 and A_2), as expected for the system close to the steady state (see comments to Figure 1). The amplitudes of $(J_{\text{loc}})_N$ and $(J_{\text{nloc}})_N$ are five times larger (see plots A_1 and A_2 in Figure 1), and both of these fluxes consist of three harmonics, zero up to second (not presented in

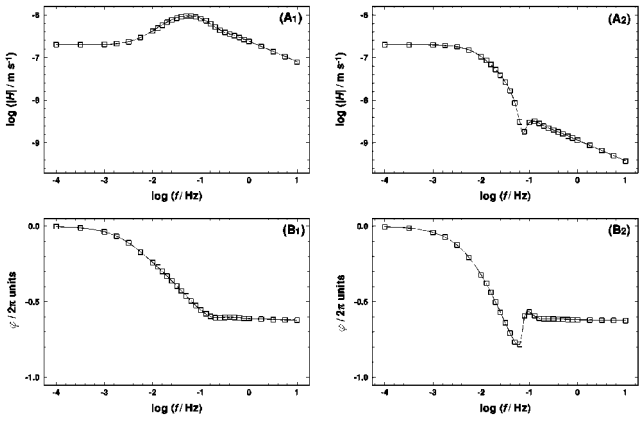

Figure 4. Spectra of the (□) nonlinear TF_f (H_{nl}, eq 21) and the (—) (linear) TF_f (H_l, eq 14) in the polar coordinates. The common parameters of the system are the same as those in Figure 1. Plots A_1 and B_1 and plots A_2 and B_2 are plotted for $c_{eq} = 2.5 \times 10^4$ and 2.5×10^2 mole m^{-3}, respectively. For H_{nl}, $\Delta c_{(0)} = 0.5 c_{eq}$.

the figures). However, for reason of their coupling, $(J_{loc})_N$ and $(J_{nloc})_N$ compensate in such a way that $(J)_N$ is as in plots A_1 and A_2 in Figure 2. At $f = 10$ Hz, $(J)_N$ consists of several Fourier terms at both specimen sides (plots B_1 and B_2 in Figure 2). At $z = L$, $(J)_N$ differs from the first harmonics mainly by the zero one (positive) (plot B_2). $(J_{nloc})_N$ is responsible for this complex structure of $(J)_N$, because $(J_{loc})_N$ consists only of the zero harmonics (plot C_2 in Figure 1). In all cases, the amplitude of the third harmonics of $(J)_N$ is not significant.

In Figure 3, the parameters P_{1har} and P_{2har} (eq 19) are plotted vs log f. The larger $\Delta c_{(0)}$, the smaller is P_{1har} and the larger is P_{2har}. For the larger and the smaller c_{eq}, P_{1har} is >91% and >99%, respectively, while always $(P_{1har} + P_{2har}) \geq 99.5\%$. At $z = 0$, the larger is log f, essentially the smaller is P_{1har} and the larger is P_{2har} (plots A_1 to C_1 in Figure 3), although at the smaller c_{eq} for P_{2har} some oscillations are noticed (plot C_1). On the contrary, at $z = L$ two distinct extremes are observed for P_{1har} and P_{2har} at $-2 < \log f < -1$ (plots A_2 to C_2 in Figure 3). For the larger c_{eq}, maximums on the dependencies of P_{3har} vs log f plots at $z = 0$ and $z = L$ close to $\log f = -2$ were noticed (not shown here). However, for no set of $\Delta c_{(0)}$ and f did P_{3har} exceed 5×10^{-3} and 5×10^{-6}, at the larger and smaller c_{eq}, respectively.

None of the extremes of P_{1har} to P_{3har} vs log f plots (e.g., see the maximum in plot C_2 in Figure 3) resulted from an implicit discontinuity of the curves. Also, no set of f, $\Delta c_{(0)}$, and c_{eq} was found for which $(J^*)_N$ could not be described reliably by the sum of the zero to third harmonics. Hence, the earlier suggestions[10,11] that an oscillating change of hydrogen concentration in the metal matrix "could be a source of interesting ... complex dissipative structures" find no corroboration.

It has to be noticed that all of the above extremes are in the region of frequencies where H_l changes its character from the diffusive (low frequencies) to the nonlocal transport (high frequencies) (see eq 14 and Figures 4 and 5).[25]

To carry on the analysis of results, one has to reformulate the definition of the flux's first harmonics from the time domain (eq 17) to the frequency domain:

$$J_{1har} = \Delta J^{c}_{1har} \exp(st) \tag{20}$$

where, in contrast to eq 17, amplitude of the first harmonics, ΔJ^{c}_{1har}, is a complex quantity.[25]

Because of eq 20, the definition of the nonlinear TF_f, H_{nl}, can be proposed on the basis of the analogy to the linearized solution of the transport equations (H_l, eq 14),[25] in which the fundamental harmonics is the only one:

$$H_{nl} = \frac{(\Delta J^{c}_{1har})_{(L)}}{\Delta c_{(0)}} \tag{21}$$

It has to be noticed that H_{nl}, defined in the space of s, in the τ space is equivalent to $(J_{1har})_N$ at $z = L$.

In Figures 4 and 5, the nonlinear TF_f (H_{nl}, eq 21) for the largest $\Delta c_{(0)}$ is plotted in the polar and rectangular coordinates, respectively, and compared with the (linear) (H_l, eq 14). The

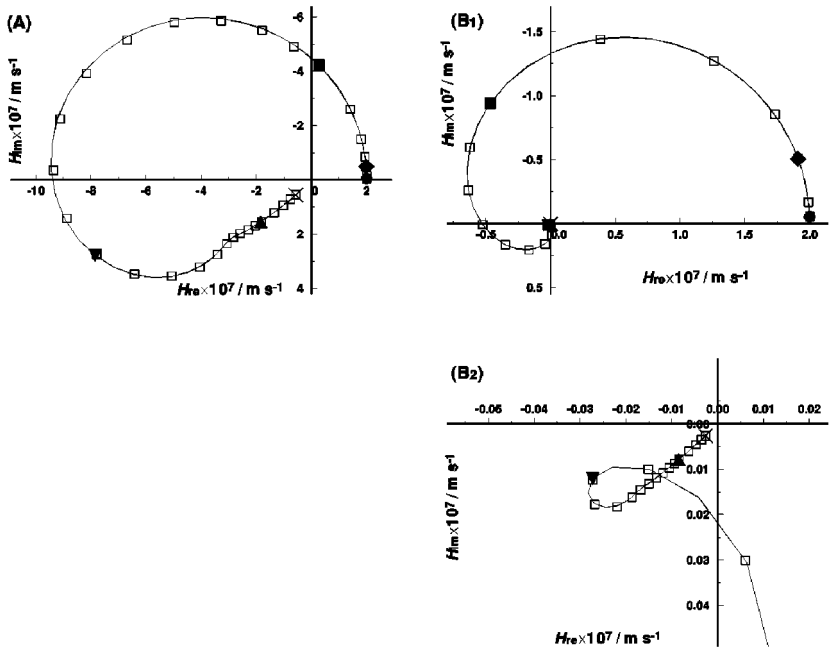

Figure 5. The same spectra as in Figure 4 in the rectangular coordinates. Plots A and B_1 are plotted for the larger and the smaller c_{eq}, respectively; plot B_2 shows a zoom of the area neighboring the coordinates' origin in plot B_1. For H_l, the decade frequencies are indicated by particular symbols: 1×10^{-4} Hz (●), 1×10^{-3} Hz (◆), 1×10^{-2} Hz (■), 1×10^{-1} Hz (▼), 1 Hz (▲), and 10 Hz (×).

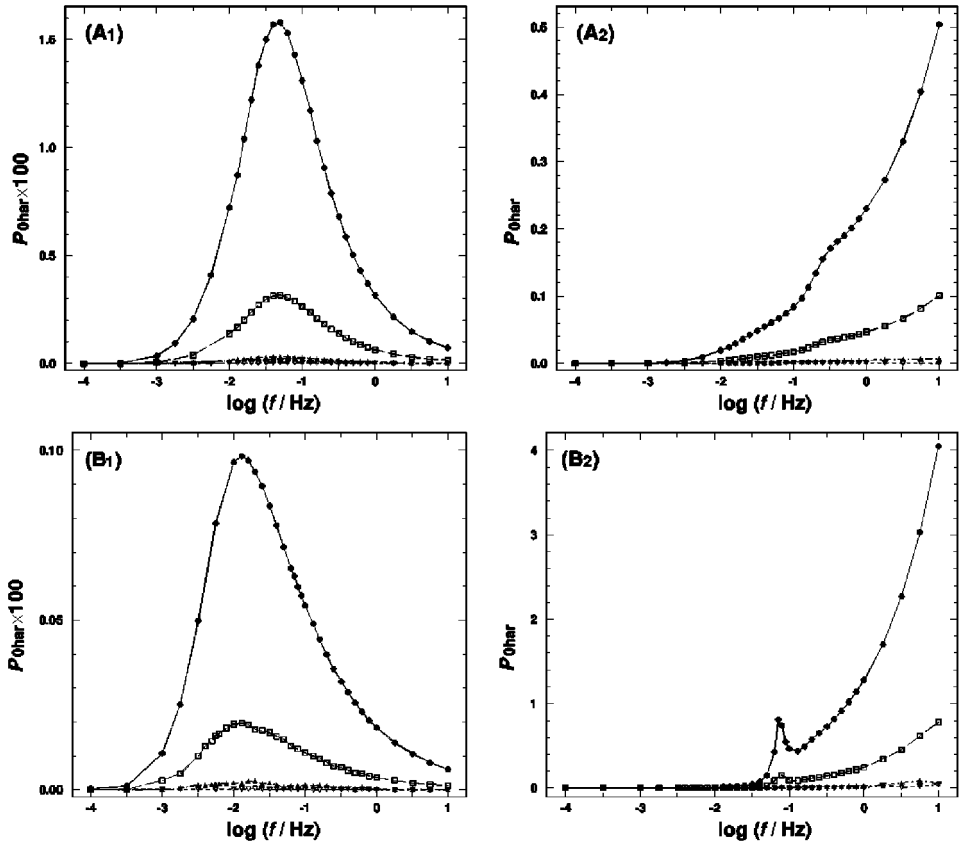

Figure 6. Plots of the ratio of the zero harmonics of the flux (J) to the root-mean-square of its higher harmonics (P_{0har}, eq 18) vs log f. Plots A_1 and B_1 and plots A_2 and B_2 are at the input and output sides of the specimen, respectively. Plots A_1 and A_2 and plots B_1 and B_2 are plotted for c_{eq} equal to 2.5×10^4 and 2.5×10^2 mole m^{-3}, respectively. Symbols for various values of $\Delta c_{(0)}$ are the same as those in Figure 3.

H_{nl} plots closely reproduce the straight-line high-frequency section of H_l (all plots in Figure 4, and plots A and B_2 in Figure 5), characteristic for the infinite diffusion (i.e., the magnitudes of real and imaginary component are equal), as well as the low-frequency section, resulting mainly from the Fickian transport. The former section results solely from the nonlocal effect of stress, and the latter is only modified to some extent by the above effect.[25] Even the peculiarities of the H_l functions in the region of frequencies, where the two sections meet each other, are closely reproduced by the H_{nl} data. Therefore, H_l appears to be a good approximation of H_{nl}.

To validate the above conclusion, the H_l model (eq 14) was fitted to the H_{nl} spectra (eq 21), using the complex nonlinear least-squares method.[45−47] All spectra consisted of three-digit values of the real and imaginary components of H_{nl} and H_l. D and $\bar{Y}$ were the only free parameters of the model. The evaluated values D and $\bar{Y}$ differed from their nominal values by $\leq 1\%$, irrespective of the values of $\Delta c_{(0)}$ and c_{eq}. This certifies that essentially the magnitude of the perturbing signal amplitude is insignificant for the evaluation of D and $\bar{Y}$.

In Figure 6, the parameter P_{0har} (eq 18) is plotted vs log f. In all cases, P_{0har} is positive. As in the case of P_{2har} (plots B_1 to C_2 in Figure 3), the larger $\Delta c_{(0)}$, the larger is P_{0har}. At $z = 0$, a large maximum of P_{0har} is observed (plots A_1 and B_1 in Figure 6). It is in the transition region of frequencies, where the high- and the low-frequency sections of H_l meet each other (see Figures 4 and 5). For the larger c_{eq}, the maximum is higher than that for the smaller one. In contrast, at $z = L$ at low frequencies, P_{0har} is close to zero, and then the higher the frequency, the larger is P_{0har} (plots A_2 and B_2 in Figure 6). Hence, P_{0har} originates from the nonlocal flux.

P_{0har}, the reciprocal of P_{1har} and P_{2har} (see Figures 3 and 6), may be treated as measures of the process nonlinearity at particular frequencies. According to all of these criteria, the larger are $\Delta c_{(0)}$ and f, the larger is the nonlinearity. However, in other aspects, the above measures are incompatible.

Obviously, the most important is P_{0har}, because it describes quantitatively a quite specific feature of nonlinearity of the transport process, namely, the appearance of the zero harmonics, this being not related only to higher harmonics. That results in a positive direct flux, that is, permanent pumping of hydrogen through the specimen. It is of real importance for TF measurements, and it may be in technology as well, because filtering of hydrogen through metal membranes is used for its purification.[33] The magnitude of the direct flux should be rated on the basis of P_{0har} at $z = 0$, because at the opposite side of the membrane P_{0har} attains the largest values at frequencies where the modulus of the TF_f is very small (see plots A_1 and A_2 in Figure 4). Therefore, in comparison with the rms of the oscillating component of the flux, the pumping of hydrogen is the largest in the transition region of frequencies where the competition between the Fickian transport and that caused by the nonlocal effect of stress is the most significant (see Figures 4 and 5, and plots A_1 and B_1 in Figure 6). The maximal value of the direct flux equals ca. 1.6% of the rms of the oscillating flux (see plot A_1 in Figure 6).

The presence of the zero harmonics is contradictory to the principles of TF.[25,26] Therefore, even when the application of a relatively small-amplitude signal is intended in the experiment, the presence of the zero harmonics should be taken into account, to fulfill the requirement that at both sides of the specimen the averaged-in-time hydrogen concentration is the same.

4. Final Remarks

This paper deals only with the bulk transport of hydrogen in the metal matrix. Therefore, all processes related to dissociative adsorption of molecular hydrogen from the gas phase at the specimen surface or to reduction of proton from a surrounding solution and to ad-, ab-, and desorption of hydrogen are either neglected or assumed to be at equilibrium. When the hindrances of surface processes are small in comparison with those of hydrogen transport inside the solid, the low-frequency part of a wide spectrum of TF may result solely from the latter.[20,24,25] Hence, when the experiments are prepared, much care should be taken to diminish the hindrances of the surface processes, and in data analysis, a possible influence of these processes should be taken into account.[10,24,25,27,48,49]

From the presented results, it may be extrapolated that also at high frequencies, relevant only from the point of view of surface processes, a constant flux will accompany the oscillating response. The nonlinearity of transport of hydrogen through a large thin metal membrane, caused by a sinusoidal perturbation of concentration at one of its sides, does not disturb significantly the measurements of TF, if the opposite side is permeable to hydrogen (TF_f's, eqs 14 and 21). However, if the opposite side of the specimen is impermeable to hydrogen, as it is in case of TF_c,[26] the existence of the zero harmonics due to the nonlinearity of transport should cause there a drift of the mean concentration of hydrogen. Therefore, for the M−H systems, in which the gradient of hydrogen results in a noticeable stress, the TF_c measurements probably cannot give reliable results.

Finally, it needs pointing out once more that the self stress should influence all phenomena of sorption of guest species in elastic host matrixes. Thus, the effects similar to those on the transport of hydrogen in metals should exist in the transport of any guest in host solids.[2,3]

5. Conclusions

(a) Because of the self stress, a periodically steady-state flux of hydrogen caused by a sinusoidal perturbation of the hydrogen concentration at one side of a large thin metallic membrane consists of an oscillating component and a constant component.

(b) The oscillating component consists mainly of the fundamental harmonics, even at large amplitude of perturbing signal. Thus, reliable values of the diffusion coefficient of hydrogen in a M−H system and of the bulk elastic modulus of the metallic solid can be obtained by the measurements of the flux transfer function taking into account only the fundamental harmonics.

(c) The constant component is positive, and it results in a permanent pumping of hydrogen throughout the membrane.

Acknowledgment. The authors thank Dr. M. Dolata and Dr. P. Kedzierzawski for important discussions.

References and Notes

(1) Schmalzried, H. *Chemical Kinetics of Solids*; VCH: Weinheim, Germany, 1995.
(2) Vakarin, E. V.; Badiali, J. P.; Levi, M. D.; Aurbach, D. *Phys. Rev. B* **2001**, *63*, 4304.
(3) Vakarin, E. V.; Badiali, J. P. *Electrochim. Acta* **2001**, *46*, 4151.
(4) McKinnon, W. R. In *Modern Aspects of Electrochemistry*; White, R. E., Bockris, J. O'M., Conway, B. E., Eds.; Plenum Press: New York, 1983; Vol. 15, p 235.
(5) Tsirlina, G. A.; Levi, M. D.; Petrii, O. A.; Aurbach, D. *Electrochim. Acta* **2001**, *46*, 4141.
(6) Lewis, F. A.; Magennis, J. P.; McKee, S. G.; Ssebuwufu, P. J. M. *Nature* **1983**, *306*, 673.
(7) Lewis, F. A.; Baranowski, B.; Kandasamy, K. *J. Less-Common Met.* **1987**, *34*, L27.
(8) Lewis, F. A.; Kandasamy, K.; Baranowski, B. *Platinum Met. Rev.* **1988**, *2*, 22.
(9) Baranowski, B.; Lewis, F. A. *Ber. Bunsen-Ges. Phys. Chem.* **1989**, *93*, 1225.
(10) Baranowski, B. *J. Less-Common Met.* **1989**, *154*, 329.
(11) Baranowski, B. In *Advances in Thermodynamics*: *Flow, Diffusion and Rate Processes*; Saniutycz, S., Salamon, P., Eds.; Taylor & Francis: New York, 1992; Vol. 6, p 168.
(12) Dudek, D.; Baranowski, B. *Pol. J. Chem.* **1995**, *69*, 1196.
(13) Kandasamy, K. *Int. J. Hydrogen Energy* **1995**, *20*, 455.
(14) Dudek, D.; Baranowski, B. *Z. Phys. Chem.* **1998**, *206*, 21.
(15) Lewis, F. A.; Kandasamy, K.; Tong, X. Q. In *Hydrogen in Metal Systems II*; Lewis, F. A., Aladjem, A., Eds.; Scitec Publications Ltd: Uetikon-Zuerich, 2000; p 207.
(16) Dudek, D. *J. Alloys Compd.* **2001**, *329*, 1.
(17) Baranowski, B.; Majchrzak S.; Flanagan, T. B. *J. Phys. F* **1971**, *1*, 258.
(18) Zhang, W.-S.; Zhang, Z.-L.; Zhang, X.-W. *J. Electroanal. Chem.* **1999**, *474*, 130.
(19) Zoltowski, P. *Electrochim. Acta* **1999**, *44*, 4415.
(20) Zoltowski, P.; Makowska, E. *Phys. Chem. Chem. Phys.* **2001**, *3*, 2935.
(21) Bruzzoni, P.; Corraza, R. M.; Collet Lacoste, J. R.; Crespo, E. A. *Electrochim. Acta* **1999**, *44*, 2693.
(22) Bruzzoni, P.; Corraza, R. M.; Collet Lacoste, J. R. *Electrochim. Acta* **1999**, *44*, 4443.
(23) Montella, C. *J. Electroanal. Chem.* **1999**, *462*, 73.
(24) Montella, C. *J. Electroanal. Chem.* **2000**, *480*, 166.
(25) Zoltowski, P. *J. Electroanal. Chem.* **2001**, *501*, 89.
(26) Zoltowski, P. *J. Electroanal. Chem.* **2001**, *512*, 64.
(27) Montella, C. *J. Electroanal. Chem.* **2002**, *518*, 61.
(28) Feenstra, R.; Griessen, R.; de Groot, D. G. *J. Phys. F* **1986**, *16*, 1933.
(29) Sakamoto, Y.; Chen, F. L.; Ura, M.; Flanagan, T. B. *Ber. Bunsen-Ges. Phys. Chem.* **1995**, *99*, 807.
(30) Górecki, T. *Mater. Sci. Eng.* **1980**, *43*, 225.
(31) Brodowsky, H. *Z. Phys. Chem. NF* **1965**, *44*, 129.
(32) Lewis, F. A. *The Palladium−Hydrogen System*; Academic Press: London, 1967.
(33) *Hydrogen in Metals II*; Alefeld, G., Völkl, J., Eds.; Springer-Verlag: Berlin, 1978.
(34) Schõneich, H.-G.; Zûchner, H. *Ber. Bunsen-Ges. Phys. Chem.* **1983**, *87*, 566.
(35) Zûchner, H.; Schõneich, H.-G. *J. Less-Common Met.* **1984**, *101*, 363.
(36) Kandasamy, K. *Scr. Metall.* **1988**, *22*, 479.
(37) Baranowski, B.; Lewis, F. A.; Majchrzak, S.; Wisniewski, R. *J. Chem. Soc., Faraday Trans. 1* **1972**, *62*, 824.
(38) Baranowski, B.; Lewis, F. A.; McFall, W. D.; Filipek, S.; Witherspoon, T. C. *Proc. R. Soc. London, Ser. A* **1983**, *386*, 309.
(39) Wicke, E.; Nernst, G. H. *Ber. Bunsen-Ges. Phys. Chem.* **1964**, *68*, 224.
(40) Bucur, R. V. *Z. Phys. Chem NF* **1985**, *146*, 217.
(41) Crank, J.; Nicolson, P. *Proc. Cambridge Philos. Soc. Math. Phys. Sci.* **1947**, *43*, 50.
(42) Li, J. C.-M. *Metall. Trans. A* **1978**, *9*, 1353.
(43) Zhang, W.-S.; Zhang, X.-W.; Zhang, Z.-L. *J. Alloys Compd.* **2000**, *302*, 258.
(44) Zhang, W.-S.; Zhang, X.-W.; Zhang, Z.-L. *Phys. Rev. B* **2000**, *62*, 8884.
(45) Macdonald, J. R.; Schoonman, J.; Lehnen, A. P. *J. Electroanal. Chem.* **1982**, *131*, 77.
(46) Zoltowski, P. *J. Electroanal. Chem.* **1984**, *178*, 11.
(47) Macdonald, J. R. *LEVM software*; Solartron: Farnborough, England, 1997.
(48) Zhang, W.-S.; Zhang, Z.-L.; Zhang, X.-W.; Wu, F. *J. Electroanal. Chem.* **1999**, *474*, 123.
(49) Zhang, W.-S.; Zhang, Z.-L.; Zhang, X.-W.; Wu, F. *J. Electroanal. Chem.* **2000**, *481*, 13.